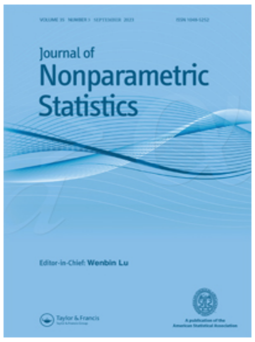

Journal of Nonparametric Statistics

ISSN: (Print) (Online) Journal homepage: https://www.tandfonline.com/loi/gnst20

Testing axial symmetry by means of integrated rank scores

Šárka Hudecová & Miroslav Šiman

JOURNAL OF NONPARAMETRIC STATISTICS
2023, VOL. 35, NO. 3, 474–490
https://doi.org/10.1080/10485252.2022.2159399

Testing axial symmetry by means of integrated rank scores

Šárka Hudecová[a] and Miroslav Šiman[b]

[a]Faculty of Mathematics and Physics, Department of Probability and Statistics, Charles University, Praha, Czech Republic; [b]Institute of Information Theory and Automation, The Czech Academy of Sciences, Praha, Czech Republic

ABSTRACT
The article addresses the recently emerging inferential problem of testing axial symmetry up to a shift, which is useful even for testing certain hypotheses of exchangeability, independence, goodness-of-fit or equality of scale. In particular, it introduces a new test of axial symmetry based on integrated rank scores for directional quantile regression. The test outperforms existing competitors in terms of size, power, robustness, moment conditions or computational feasibility. All that is illustrated with a series of simulated examples.

ARTICLE HISTORY
Received 15 June 2022
Accepted 10 December 2022

KEYWORDS
Axial symmetry; symmetry around a line; exchangeability; directional quantile; quantile regression

AMS SUBJECT CLASSIFICATIONS
MSC 62H15; MSC 62G10

1. Introduction

This article deals with nonparametric testing of symmetry around a line in a given direction. From the mathematical point of view, stochastic vector $\boldsymbol{Y} \in \mathbb{R}^m$, $m \geq 2$, is axially symmetric around an axis with direction $\boldsymbol{u} \in \mathbb{R}^m$ when $\mathcal{L}\{\boldsymbol{Y} - \mathrm{E}\boldsymbol{Y}\} = \mathcal{L}\{\mathbf{R}(\boldsymbol{Y} - \mathrm{E}\boldsymbol{Y})\}$ for the rotational (orthonormal) reflection matrix $\mathbf{R} = 2\mathbf{u}\mathbf{u}^\top - \mathbf{I}$.

The tests of axial symmetry may also be useful for testing certain exchangeability, independence, goodness-of-fit and equality-of-scale hypotheses, as explained and illustrated with simulated and real data examples in Hudecová and Šiman (2021a) or Hudecová and Šiman (2021b). They might also be useful in full generality because axial symmetry naturally occurs (not only) whenever mirrors or reflections are employed.

Nonparametric tests of symmetry around a general line already exist in the bivariate case when axial symmetry and halfspace symmetry coincide (Rao and Raghunath 2012). See also Hollander (1971) and Modarres (2008) for some examples of (bivariate) nonparametric tests of exchangeability that use a particular axis of symmetry, namely the axis of the first quadrant. Furthermore, the tests of (multivariate) conditional symmetry with a scalar conditioning variable also test axial symmetry of the joint distribution around the coordinate axis corresponding to the conditioning variable; see, e.g. Riahi and Patil (2021), or the kernel-based nonparametric test of Su (2006) and references given there.

CONTACT Šárka Hudecová hudecova@karlin.mff.cuni.cz Faculty of Mathematics and Physics, Department of Probability and Statistics, Charles University, Sokolovská 83, Praha 186 75, Czech Republic

In spaces of arbitrary dimension, Kalina (2021) tested the axial symmetry hypothesis by means of certain permutation tests without desirable invariance properties. Furthermore, Hudecová and Šiman (2021a) introduced some nonparametric asymptotic tests of the hypothesis in a general regression setup. They are based on the directional quantile regression of Hallin, Paindaveine, and Šiman (2010), naturally invariant, free of restrictive distributional assumptions, and consistent in the class of all elliptical distributions even for a single quantile level. Unfortunately, the most powerful tests of them are poorly sized and have a complex null asymptotic distribution whose critical values or p-values are impossible to determine accurately if the dimension of observations is large.

Finally, Hudecová and Šiman (2021b) came up with some parametric, nonparametric, permutation and asymptotic naturally invariant tests of the more general hypothesis of symmetry around a shifted subspace, but only in the purely multivariate (non-regression) case. The tests employ canonical or rank correlations. Although their parametric variants are practical only for elliptical distributions and require quite stringent moment conditions, they have simple null asymptotic distributions and may be more powerful than all the tests of Hudecová and Šiman (2021a).

This work introduces a new test of axial symmetry that is defined by means of integrated rank scores. Although it stems from the directional quantile regression like the tests of Hudecová and Šiman (2021a), it appears not to share their drawbacks, namely low power, inaccurate size for small samples and complicated asymptotic distribution not tractable in large dimensions. In particular, the power of the new test with the van der Waerden or Wilcoxon scores reaches that of its most powerful competitors of Hudecová and Šiman (2021b). Other scores may be useful in the presence of outliers or if some information about the underlying distribution is available in advance.

In what follows, Section 2 presents the notation and summarises useful relevant results, and Section 3 introduces the new test and derives its null asymptotic distribution for various score functions. Section 4 explores the proposed test in terms of finite sample behaviour and compares it to other general tests of axial symmetry, while Section 5 is focusing on size and power comparisons with some rather specific tests in the bivariate case. The last Section 6 collects concluding comments. The proofs, figures, and tables are provided in Appendices 1–3, respectively.

2. Definitions and preliminary considerations

Let $\mathbf{Y}$ be an m-dimensional real vector satisfying

Assumption 2.1: The distribution $\mathcal{L}(\mathbf{Y})$ of $\mathbf{Y}$ is absolutely continuous with finite expectation, cumulative distribution function F, and probability density function f that is continuous, bounded, and positive in the interior of a connected support.

Hudecová and Šiman (2021a) proved that the null hypothesis

$$H_0^S(\mathbf{u}):\ \mathcal{L}(\mathbf{Y}) \text{ is axially symmetric around a line in unit direction } \mathbf{u} \in \mathbb{R}^m$$

always implies

$$H_0(\mathbf{u}):\ \boldsymbol{\gamma}_\tau = \mathbf{0} \quad \text{for all } \tau \in (0,1)$$

where $(\boldsymbol{\gamma}_\tau^\top, \alpha_\tau)^\top$ by definition minimises

$$\min_{(\boldsymbol{\gamma}^\top,\alpha)^\top \in \mathbb{R}^m} \mathrm{E}\rho_\tau(\mathbf{u}^\top \mathbf{Y} - \boldsymbol{\gamma}^\top \Gamma_{\mathbf{u}}^\top \mathbf{Y} - \alpha) \tag{1}$$

with $\Gamma_{\mathbf{u}}$ being an $m \times (m-1)$ matrix complementing $\mathbf{u}$ to an orthonormal matrix. That article also proved that $H_0(\mathbf{u})$ implies $H_0^S(\mathbf{u})$ in the class of elliptical distributions where $\boldsymbol{\gamma}_\tau = \mathbf{0}$ either for all $\tau \in (0, 1)$ or for none of them.

Consider also n independent copies $\mathbf{Y}_1, \ldots, \mathbf{Y}_n$ of $\mathbf{Y}$ and write $\mathbb{Y} = (\mathbf{Y}_1, \ldots, \mathbf{Y}_n)^\top$. Define rank score vector $\widehat{\mathbf{a}}(\tau) = (\widehat{a}_1(\tau), \ldots, \widehat{a}_n(\tau))^\top$,

$$\widehat{\mathbf{a}}(\tau) = \operatorname{argmax}\{\mathbf{u}^\top \mathbb{Y}^\top \mathbf{a} : \ n^{-1}\mathbf{1}_n^\top \mathbf{a} = (1-\tau), \ \mathbf{a} \in [0,1]^n\},$$

and integrated rank score vector $\widehat{\mathbf{b}} = (\widehat{b}_1, \ldots, \widehat{b}_n)^\top$ with

$$\widehat{b}_i = -\int_0^1 \phi(t)\,\mathrm{d}\widehat{a}_i(t) = \phi(0) + \int_0^1 \widehat{a}_i(t)\,\mathrm{d}\phi(t) \tag{2}$$

where the last equality holds because the (score) function ϕ is required here to meet the following assumption:

Assumption 2.2: Function $\phi : [0, 1] \to \mathbb{R}$ is a square-integrable and non-decreasing real function constant outside $[\varepsilon, 1-\varepsilon]$ for some $\varepsilon > 0$. (Then also $\bar{\phi} := \int_0^1 \phi(t)\,\mathrm{d}t < \infty$.)

For example, $\phi(t) = \operatorname{sign}(t - 0.5)$ results in the sign (or, median) scores, $\phi(t) = t - 0.5$ generates the Wilcoxon scores, and ϕ equal to the quantile function of the standard normal distribution leads to the normal (or, van der Waerden) scores. In fact, the normal quantile function should be changed to a constant outside the $[\epsilon, 1-\varepsilon]$ interval to comply with Assumption 2.2 but ε may be always small enough to make no practical difference. Therefore, the simulation studies below do not distinguish between the two cases.

3. Theory

Articles Gutenbrunner and Jurečková (1992) and Gutenbrunner, Jurečková, Koenker, and Portnoy (1993) already defined (integrated) rank scores and employed them for testing whether certain regression coefficients are zero in quantile regression models with deterministic regressors. This article suggests to follow their approach and to use their test statistic even for testing $\boldsymbol{\gamma}_\tau = \mathbf{0}$ in the quantile regression model behind (1) when the regressors are stochastic and possibly dependent on the response. This complicates the matter and requires a new proof regarding the asymptotic null distribution of the test statistic; see Appendix A.

Proposition 3.1: *Consider test statistic*

$$\widehat{\mathbf{S}}_n = \frac{1}{\sqrt{n}} \sum_{i=1}^{n} \Gamma_{\mathbf{u}}^\top (\mathbf{Y}_i - \overline{\mathbf{Y}})\widehat{b}_i, \tag{3}$$

suppose that Assumptions 2.1 *and* 2.2 *hold with* $\mathrm{E}\|\boldsymbol{Y}\|^{2+\delta} < \infty$ *for some* $\delta > 0$, *and assume that* $H_0^S(\mathbf{u})$ *is true. Then, as* $n \to \infty$,

$$\widehat{\mathbf{S}}_n \xrightarrow{D} \mathsf{N}(\mathbf{0}, \boldsymbol{\Sigma}) \quad \textit{and} \quad \widehat{\mathbf{S}}_n^\top \boldsymbol{\Sigma}^{-1} \widehat{\mathbf{S}}_n \xrightarrow{D} \chi^2_{m-1}$$

where

$$\boldsymbol{\Sigma} = \mathrm{E}\{[\phi(F_{\mathbf{u}}(\mathbf{u}^\top \mathbf{Y})) - \bar{\phi}]^2 \Gamma_{\mathbf{u}}^\top (\mathbf{Y} - \mathrm{E}\mathbf{Y})(\mathbf{Y} - \mathrm{E}\mathbf{Y})^\top \Gamma_{\mathbf{u}}\} \tag{4}$$

and $F_{\mathbf{u}}$ *is the cumulative distribution function of* $\mathbf{u}^\top \mathbf{Y}$.

As a consequence, $H_0^S(\mathbf{u})$ may be tested by means of the test statistic

$$T_n := \widehat{\mathbf{S}}_n^\top \widehat{\boldsymbol{\Sigma}}^{-1} \widehat{\mathbf{S}}_n \xrightarrow{D} \chi^2_{m-1} \tag{5}$$

where

$$\widehat{\boldsymbol{\Sigma}} = \frac{1}{n} \sum_{i=1}^{n} [\phi(\widehat{F}_{\mathbf{u}}(\mathbf{u}^\top \mathbf{Y}_i)) - \bar{\phi}]^2 \Gamma_{\mathbf{u}}^\top (\mathbf{Y}_i - \overline{\mathbf{Y}})(\mathbf{Y}_i - \overline{\mathbf{Y}})^\top \Gamma_{\mathbf{u}}$$

is a consistent estimator of $\boldsymbol{\Sigma}$ using a consistent empirical counterpart $\widehat{F}_{\mathbf{u}}$ to $F_{\mathbf{u}}$ such as the empirical cummulative distribution function.

Remark 3.1: The original (integrated) rank score χ^2-test of Gutenbrunner et al. (1993), known from the standard quantile regression and implemented in various software, uses almost the same test statistic but with the sample matrix estimator $\widehat{\boldsymbol{\Sigma}}_0$ of

$$\boldsymbol{\Sigma}_0 := \mathrm{Var}\,(\Gamma_{\mathbf{u}}^\top \mathbf{Y}) \int_0^1 [\phi(t) - \bar{\phi}]^2 \,\mathrm{d}t.$$

Consequently, the test remains valid in the present context only in certain special cases when $\widehat{\boldsymbol{\Sigma}}_0 = \widehat{\boldsymbol{\Sigma}} + o_P(1)$, e.g. if $\Gamma_{\mathbf{u}}^\top \mathbf{Y}$ and $\mathbf{u}^\top \mathbf{Y}$ are independent, or if the sign score function is employed.

Remark 3.2: If $\phi(t) = 0.5\,\mathrm{sign}(t - 0.5)$, then $\widehat{\mathbf{b}} = \widehat{\mathbf{a}}(0.5) - \mathbf{1}_n$ and the test T_n of (5) exactly coincides with the χ^2 test of (4.4) in Hudecová and Šiman (2021a) for $k = 1$ and $\tau_1 = 0.5$.

Remark 3.3: Note also that the test statistic $T_n = T_n(\mathbf{u}, \mathbb{Y}, \Gamma_{\mathbf{u}})$ of (5),

$$T_n = \frac{1}{n} \widehat{\mathbf{b}}^\top \left(\mathbf{I} - \frac{1}{n}\mathbf{1}\mathbf{1}^\top\right) \mathbb{Y} \Gamma_{\mathbf{u}} \widehat{\boldsymbol{\Sigma}}^{-1} \Gamma_{\mathbf{u}}^\top \mathbb{Y}^\top \left(\mathbf{I} - \frac{1}{n}\mathbf{1}\mathbf{1}^\top\right)^\top \widehat{\mathbf{b}}, \tag{6}$$

inherits favourable invariance and equivariance properties from the tests in Hudecová and Šiman (2021a). In particular, T_n is independent of the choice of $\Gamma_{\mathbf{u}}$ and naturally invariant with respect to linear transformations preserving axial symmetry, namely to certain shift, rotation and linear scale transformations:

$$\begin{aligned} T_n(\mathbf{u}, \mathbb{Y}, \Gamma_{\mathbf{u}}) &= T_n(\mathbf{u}, \mathbb{Y} - \mathbf{s}^\top \mathbf{1}_n, \Gamma_{\mathbf{u}}) = T_n(\mathbf{A}\mathbf{u}, \mathbb{Y}\mathbf{A}^\top, \mathbf{A}\Gamma_{\mathbf{u}}) \\ &= T_n(\mathbf{u}, \mathbb{Y}(\mathbf{u}|\Gamma_{\mathbf{u}})\mathbf{D}(\mathbf{u}|\Gamma_{\mathbf{u}})^\top, \Gamma_{\mathbf{u}}) \end{aligned}$$

for any vector $\mathbf{s} \in \mathbb{R}^m$, any orthonormal (i.e. rotational) $m \times m$ matrix $\mathbf{A}$, and any $m \times m$ diagonal matrix $\mathbf{D} = \mathrm{diag}(d_{11}, \ldots, d_{mm})$ with $d_{11} > 0$. The equalities can be obtained directly from (6).

Remark 3.4: The test of (5) is consistent in the class of elliptically symmetric distributions according to what is written in Section 2. It is also sensitive to many other alternatives, though not against all.

Remark 3.5: The computation of T_n can be done easily, e.g. in the *R* computational environment (R Core Team 2021) with the aid of the quantreg package (Koenker 2015) and its functions *qr* and *ranks*.

Note also that if ϕ is (a trimmed version of) the quantile function of the standard normal distribution and if the assumptions of Proposition 3.1 hold, then $\mathbf{\Sigma}$ of (4) can be consistently estimated by means of

$$\widehat{\mathbf{\Sigma}} = \frac{1}{n}\sum_{i=1}^{n}[\phi(\widehat{F}_{\mathbf{u}}(\mathbf{u}^\top \mathbf{Y}_i) - 0.5/n) - \bar{\phi}]^2 \Gamma_{\mathbf{u}}^\top (\mathbf{Y}_i - \overline{\mathbf{Y}})(\mathbf{Y}_i - \overline{\mathbf{Y}})^\top \Gamma_{\mathbf{u}},$$

where the correction term $0.5/n$ makes no asymptotic difference but simplifies the computation of the van der Waerden scores considerably.

Remark 3.6: Proposition 3.1 with (5) defines one test with many variants that depend on the choice of the score function and lead to the same asymptotic null distribution. The Wilcoxon and van der Waerden scores are known to be asymptotically optimal in the case of deterministic regressors for the logistic and normal distributions, respectively (Gutenbrunner et al. 1993). The sign scores are useful in the same context in the presence of outliers or heavy tails. This is the reason why these three types of scores are employed in the following simulation study focusing on the the behaviour of the new test.

4. Empirical study

This section uses simulations to explore the proposed test (5), to investigate its finite sample performance for various score functions and data distributions, and to compare it to the representative tests of Hudecová and Šiman (2021a) and Hudecová and Šiman (2021b) that are used for benchmarking here. To the best of our knowledge, there are no other competitors suitable for comparison beyond dimension two. In addition, the benchmark tests themselves have already been shown to clearly outperform the closest competitor in the bivariate case (Rao and Raghunath 2012), see Hudecová and Šiman (2021b).

In particular, three benchmark tests are considered:

- T_C: the χ^2 Wilks correlation test based on (1) and (2) of Hudecová and Šiman (2021b),
- T_R: the χ^2 rank test based on (6) of Hudecová and Šiman (2021b),
- T_{sup}: the sup-based non-χ^2 test based on (4.5) of Hudecová and Šiman (2021a),

and the following tests based on integrated rank scores are used for comparison:

- T_N: the χ^2 test of (5) with normal scores,
- T_S: the χ^2 test of (5) with sign scores,
- T_W: the χ^2 test of (5) with Wilcoxon's scores,

and also their variants T_{N0}, T_{S0}, and T_{W0} using $\widehat{\Sigma}_0$ of Remark 3.1 instead of $\widehat{\boldsymbol{\Sigma}}$, although only the T_{N0} variant is also presented in the graphical output for the sake of brevity.

Note that the particular tests T_C and T_R work only for elliptical distributions, that T_C also requires finite sixth moments, and that $T_{\sup}$ assumes rather special conditions to be fulfilled such as normally distributed data. All that had to be taken into consideration in the simulations.

The simulation experiments behind all figures were conducted in the *R* computational environment (R Core Team 2021). Each experiment used 1000 independent m-dimensional random samples of size n and tested them individually for symmetry around a line in direction $\mathbf{u} = (\cos(\alpha), \sin(\alpha), \mathbf{0}^\top)^\top, \alpha \in [0, \pi/6]$. The null hypothesis always corresponds (only) to $\alpha = 0$. The results are reported in terms of average sample p-values and their plots against α. Recall that the average p-values should concentrate around 0.5 under the null hypothesis and decrease with α. The most powerful test corresponds to that with the lowest average p-values for $\alpha > 0$.

The most interesting findings are presented in Figures A1 to A9. As the graphical outputs for various tests often lie close to one another, each plot displays at most three of them to prevent confusion.

Basically, Figure A1 focuses on the comparison with $T_{\sup}$, Figure A2 on the comparison with T_C, Figure A3 on the use of different score functions, Figure A4 on small samples, Figure A5 on elliptical distributions with finite sixth moments, Figure A6 on elliptical distributions with infinite sixth moments and on the comparison with T_R, Figure A7 on the influence of outliers, Figure A8 on large large-dimensional samples, and Figure A9 on the difference between using $\widehat{\boldsymbol{\Sigma}}$ and $\widehat{\Sigma}_0$.

Usually $n = 100$, although $n = 25$ is used in the small-sample study of Figure A4 and $n = 1000$ is employed in the large-sample study of Figure A8. Similarly, $m = 3$ as a rule although $m = 100$ is used in the large-dimensional (and large-sample) study of Figure A8 and $m = 10$ is employed in Figure A3 to show what happens when the dimension is changed from small to moderate.

To sum up the results:

- Figure A1 compares $T_{\sup}$, T_N, and T_W on random samples containing $n = 100$ three-dimensional observations $(Y_1, 2Y_2, 3Y_3)^\top$ whose distribution has independent marginals. In particular, Y_i's, $i = 1, \ldots, 3$, are standard normal, uniform on $(0, 1)$, standard exponential, or standard logistic.
- Figure A2 compares T_C, $T_{\sup}$, and T_N on random samples containing $n = 100$ three-dimensional elliptically distributed observations $(Y_1, 2Y_2, 3Y_3)^\top$ where the distribution of $(Y_1, Y_2, Y_3)^\top$ is multivariate standard normal, multivariate canonical Laplace, or multivariate canonical Student with 7 degrees of freedom. The use of $T_{\sup}$ is justified only for the normal distribution.
- Figure A3 compares T_N, T_S, and T_W on random samples containing $n = 100$ observations $(Y_1, 2Y_2, \ldots, 10Y_{10})^\top$ of dimension $m = 10$ where the distribution of $(Y_1, \ldots, Y_{10})^\top$ is multivariate standard normal.
- Figure A4 compares T_C, T_R, and T_N on small samples containing $n = 25$ three-dimensional observations $(Y_1, 2Y_2, 3Y_3)^\top$ where the distribution of $(Y_1, Y_2, Y_3)^\top$ is multivariate standard normal.

- Figure A5 compares T_C, T_N, and T_W on random samples containing $n = 100$ three-dimensional elliptically distributed observations $(Y_1, 2Y_2, 3Y_3)^\top$ where the distribution of $(Y_1, Y_2, Y_3)^\top$ is multivariate standard normal, multivariate canonical Student with 7 degrees of freedom, multivariate canonical Laplace, or multivariate canonical power exponential with kurtosis parameter $\kappa = 0.2$.
- Figure A6 compares T_R, T_N, and T_W on random samples containing $n = 100$ three-dimensional elliptically distributed observations $(Y_1, 2Y_2, 3Y_3)^\top$ where the distribution of $(Y_1, Y_2, Y_3)^\top$ is heavy-tailed, namely multivariate canonical Student with 3 or 5 degrees of freedom.
- Figure A7 compares T_C, T_{sup}, T_N, T_S, and T_W on contaminated normal random samples containing $n = 100$ three-dimensional observations $(Y_1, 2Y_2, 3Y_3)^\top$ where the distribution of $(Y_1, Y_2, Y_3)^\top$ is multivariate standard normal but each coordinate of the first two observations is increased by 3.
- Figure A8 compares T_N, T_S, and T_W on large high-dimensional random samples containing $n = 1000$ observations $(Y_1, 2Y_2, \dots, 100Y_{100})^\top$ of dimension $m = 100$ where the distribution of $(Y_1, \dots, Y_{100})^\top$ is multivariate standard normal.
- Figure A9 compares T_{N0} and T_N on random samples containing $n = 100$ three-dimensional observations $(Y_1, 2Y_2, 3Y_3)^\top$ where the distribution of $(Y_1, \dots, Y_3)^\top$ is multivariate standard normal or multivariate canonical Student with 7 degrees of freedom.

All the results can be summarised as follows:

- T_N, T_S and T_W are usually better sized than T_{sup},
- T_N and T_W are usually more powerful than T_{sup},
- T_N behaves like T_C for elliptical distributions,
- T_R outperforms T_N in terms of power only for heavy-tailed elliptical distributions,
- T_N, T_S and T_W can be used even for samples of small length such as $n = 25$,
- T_N and T_W often behave similarly in terms of size and power, though T_W seems more powerful for heavy-tailed distributions and less powerful otherwise,
- T_S is often less powerful than T_N and T_W,
- T_S is more robust to shift outliers than T_W, T_N, T_C and T_{sup},
- T_N, T_S and T_W are applicable and correctly sized even in case of large samples of high-dimensional observations
- the tests of (5) using $\widehat{\boldsymbol{\Sigma}}$ are only very marginally worse than those using $\widehat{\boldsymbol{\Sigma}}_0$ in the rare cases when both estimators can be used.

To sum up, T_N can be recommended as a general test of multivariate axial symmetry for all distributions with finite third-order moments. Test T_S appears suitable only in the presence of outliers. The tests using other score functions may be useful if more information about the underlying distribution is available. For example, T_W seems preferable for heavy-tailed distributions.

Even in case of elliptical distributions, T_N is virtually as powerful as T_C. Furthermore, T_N is significantly outperformed by T_R only in case of very heavy-tailed distributions when a special trimmed score function (such as one derived from the quantile function of a heavy-tailed Student distribution) could easily remove the handicap.

5. Power comparison in the bivariate case

Section 4 demonstrates that the proposed test (5) generally outperforms the benchmark tests employed. Hudecová and Šiman (2021a) and Hudecová and Šiman (2021b) show in the bivariate case that the benchmarks are generally superior to the RR_k test of axial symmetry of Rao and Raghunath (2012) that was ibidem also compared to a few comparable bivariate tests in some small sample experiments. Therefore, it seems safe to conclude that the test based on (5) performs well even with respect to the bivariate competitors.

Recently, Riahi and Patil (2021) proposed a test of symmetry around the x-axis in the bivariate case. In their simulation study, the authors considered also the following null hypotheses H_0^{UNI} and $H_0^{\mathrm{BVN}(0)}$:

$$H_0^{\mathrm{UNI}} : X \sim U[-1,1] \text{ independent of } Y \sim U[-1,1], \quad \text{and}$$
$$H_0^{\mathrm{BVN}(0)} : X \sim N(0,1) \text{ independent of } Y \sim N(0,1),$$

and four alternatives $H_1^{\mathrm{BVN}(0.3)}$, $H_1^{\mathrm{BVN}(0.6)}$, H_1^{UXM}, and H_1^{HAM}, where

$$H_1^{\mathrm{BVN}(\rho)} : (X,Y)^\top \text{ is bivariate normal with correlation } \rho, X \sim N(0,1), \text{ and } Y \sim N(0,1),$$
$$H_1^{\mathrm{UXM}} : X \sim U[0,1] \text{ independent of } Y \sim Exp(1) - \ln(2), \quad \text{and}$$
$$H_1^{\mathrm{HAM}} : X \sim Exp(1) - 1 \text{ independent of } Y \sim Exp(1) - \ln(2).$$

The test statistics T_{N0}, T_N, T_{S0}, T_S, T_{W0}, and T_W were applied to the same setting and their empirical sizes and powers, based on 100, 000 independent replications, can be found in Tables A1 and A2 for various sample sizes $n = 50, 60, 75, 100$ and 150. Table A1 also includes the empirical sizes and powers of tests $RR_{k=2}$, $RR_{k=5}$ and EG from Riahi and Patil (2021), computed therein from 1000 replications.

Table A1 confirms that the test of (5) is generally superior to any of the bivariate tests $RR_{k=2}$, $RR_{k=5}$ and EG both in terms of size and power. Table A2 then illustrates Remark 3.4 by presenting the results for two alternatives with respect to which the test of (5) is not consistent.

6. Concluding remarks

This article introduced some tests of axial symmetry based on integrated rank scores. The test based on the van der Waerden scores appears the best for general testing of multivariate axial symmetry out of all the tests currently available. It is usually quite powerful, correctly sized, reasonably invariant and applicable to all multivariate distributions under very mild conditions.

Acknowledgements

The authors would like to thank the editor and two anonymous reviewers for their valuable comments.

Disclosure statement

The authors report there are no competing interests to declare.

Funding

The research of Miroslav Šiman was supported by the Czech Science Foundation project GA21-05325S. The research of Šárka Hudecová was supported by the Czech Science Foundation project GAČR 22–01639K.

References

Einmahl, J., and Gan, Z. (2016), 'Testing for Central Symmetry', *Journal of Statistical Planning and Inference*, 169, 27–33.
Gutenbrunner, C., and Jurečková, J. (1992), 'Regression Rank Scores and Regression Quantiles', *Annals of Statistics*, 20, 305–330.
Gutenbrunner, C., Jurečková, J., Koenker, R., and Portnoy, S. (1993), 'Tests of Linear Hypotheses Based on Regression Rank Scores', *Journal of Nonparametric Statistics*, 2, 307–331.
Hallin, M., Paindaveine, D., and Šiman, M. (2010), 'Multivariate Quantiles and Multiple-Output Regression Quantiles: From L_1 Optimization to Halfspace Depth', *Annals of Statistics*, 38, 635–669.
Hollander, M. (1971), 'A Nonparametric Test for Bivariate Symmetry', *Biometrika*, 58, 203–212.
Hudecová, Š., and Šiman, M. (2021a), 'Testing Axial Symmetry by Means of Directional Regression Quantiles', *Electronic Journal of Statistics*, 15, 2690–2715.
Hudecová, Š., and Šiman, M. (2021b), 'Testing Symmetry Around a Subspace', *Statistical Papers*, 62, 2491–2508.
Kalina, J. (2021), 'Common Multivariate Estimators of Location and Scatter Capture the Symmetry of the Underlying Distribution', *Communications in Statistics – Simulation and Computation*, 50, 2485–2857.
Koenker, R. (2015), *quantreg: Quantile Regression*. R package.
Modarres, R. (2008), 'Tests of Bivariate Exchangeability', *International Statistical Review*, 76, 203–213.
R Core Team (2021), *R: A Language and Environment for Statistical Computing*, R Foundation for Statistical Computing, Vienna, Austria. Available at https://www.R-project.org.
Rao, K.S.M., and Raghunath, M. (2012), 'A Simple Nonparametric Test for Bivariate Symmetry About a Line', *Journal of Statistical Planning and Inference*, 142, 430–444.
Riahi, S., and Patil, P.N. (2021), 'Testing for Central Symmetry and Symmetry About An Axis', *Communications in Statistics – Simulation and Computation*, in press. Available at https://doi.org/10.1080/03610918.2020.1866204.
Su, L. (2006), 'A Simple Test for Multivariate Conditional Symmetry', *Economics Letters*, 93, 374–378.

Appendices

Appendix 1. Proofs

Proof of Proposition 3.1: It follows from (2), (3), and the definition of $\widehat{\mathbf{a}}(\tau)$ that $\widehat{\mathbf{S}}_n = \int_0^1 -\phi(\tau)\,\mathrm{d}\widehat{\mathbf{V}}_n(\tau)$ for

$$\widehat{\mathbf{V}}_n(\tau) = \frac{1}{\sqrt{n}}\sum_{i=1}^{n}\Gamma_{\mathbf{u}}^{\top}(\mathbf{Y}_i - \overline{\mathbf{Y}})(\widehat{a}_i(\tau) - 1 + \tau).$$

Furthermore, it is proved in Hudecová and Šiman (2021a) that $\widehat{\mathbf{V}}_n(\tau) = \mathbf{V}_n^0(\tau) + \boldsymbol{R}_n(\tau)$, where

$$\mathbf{V}_n^0(\tau) = \frac{1}{\sqrt{n}}\sum_{i=1}^{n}\Gamma_{\mathbf{u}}^{\top}(\mathbf{Y}_i - \mathrm{E}\mathbf{Y})(\mathrm{I}[\mathbf{u}^{\top}\mathbf{Y}_i > F_{\mathbf{u}}^{-1}(\tau)] - 1 + \tau),$$

$F_{\mathbf{u}}^{-1}(\tau)$ is the τ-quantile of $\mathbf{u}^{\top}\mathbf{Y}$, and $\|\boldsymbol{R}_n(\tau)\| \to 0$ uniformly in $\tau \in [\varepsilon, 1-\varepsilon]$.

Consequently, $\widehat{\mathbf{S}}_n = \int_0^1 -\phi(\tau) d\mathbf{V}_n^0(\tau) + o_P(1)$ and

$$\int_0^1 -\phi(\tau)\,\mathrm{d}\mathbf{V}_n^0(\tau) = \frac{1}{\sqrt{n}} \sum_{i=1}^n \Gamma_{\mathbf{u}}^\top (\mathbf{Y}_i - \mathrm{E}\mathbf{Y}) \left[\int_0^1 \phi(\tau)\,\mathrm{dI}[\mathbf{u}^\top \mathbf{Y}_i < F_{\mathbf{u}}^{-1}(\tau)] - \bar{\phi} \right]$$

$$= \frac{1}{\sqrt{n}} \sum_{i=1}^n \Gamma_{\mathbf{u}}^\top (\mathbf{Y}_i - \mathrm{E}\mathbf{Y}) \left[\phi(F_{\mathbf{u}}(\mathbf{u}^\top \mathbf{Y}_i)) - \bar{\phi} \right] = \frac{1}{\sqrt{n}} \sum_{i=1}^n \mathbf{Z}_i$$

where $\mathbf{Z}_i := \Gamma_{\mathbf{u}}^\top (\mathbf{Y}_i - \mathrm{E}\mathbf{Y})[\phi(F_{\mathbf{u}}(\mathbf{u}^\top \mathbf{Y}_i)) - \bar{\phi}]$, $i = 1, \ldots, n$, are independent and identically distributed random vectors.

Vectors $(\mathbf{u}^\top(\mathbf{Y} - \mathrm{E}\mathbf{Y}), (\mathbf{Y} - \mathrm{E}\mathbf{Y})^\top \Gamma_{\mathbf{u}})^\top$ and $(\mathbf{u}^\top(\mathbf{Y} - \mathrm{E}\mathbf{Y}), -(\mathbf{Y} - \mathrm{E}\mathbf{Y})^\top \Gamma_{\mathbf{u}})^\top$ are equally distributed under $H_0^S(\mathbf{u})$, and thus

$$\mathrm{E}\mathbf{Z}_i = \mathrm{E}\Gamma_{\mathbf{u}}^\top (\mathbf{Y} - \mathrm{E}\mathbf{Y})[\phi(F_{\mathbf{u}}(\mathbf{u}^\top \mathbf{Y})) - \bar{\phi}] = -\mathrm{E}\Gamma_{\mathbf{u}}^\top (\mathbf{Y} - \mathrm{E}\mathbf{Y})[\phi(F_{\mathbf{u}}(\mathbf{u}^\top \mathbf{Y})) - \bar{\phi}],$$

which implies $\mathrm{E}\mathbf{Z}_i = \mathbf{0}$. Furthermore,

$$\mathrm{Var}\,\mathbf{Z}_1 = \mathrm{E}\mathbf{Z}_1\mathbf{Z}_1^\top = \mathrm{E}\left\{ [\phi(F_{\mathbf{u}}(\mathbf{u}^\top \mathbf{Y})) - \bar{\phi}]^2 \Gamma_{\mathbf{u}}^\top (\mathbf{Y} - \mathrm{E}\mathbf{Y})(\mathbf{Y} - \mathrm{E}\mathbf{Y})^\top \Gamma_{\mathbf{u}} \right\},$$

and the rest follows from the central limit theorem. ■

Appendix 2. Figures

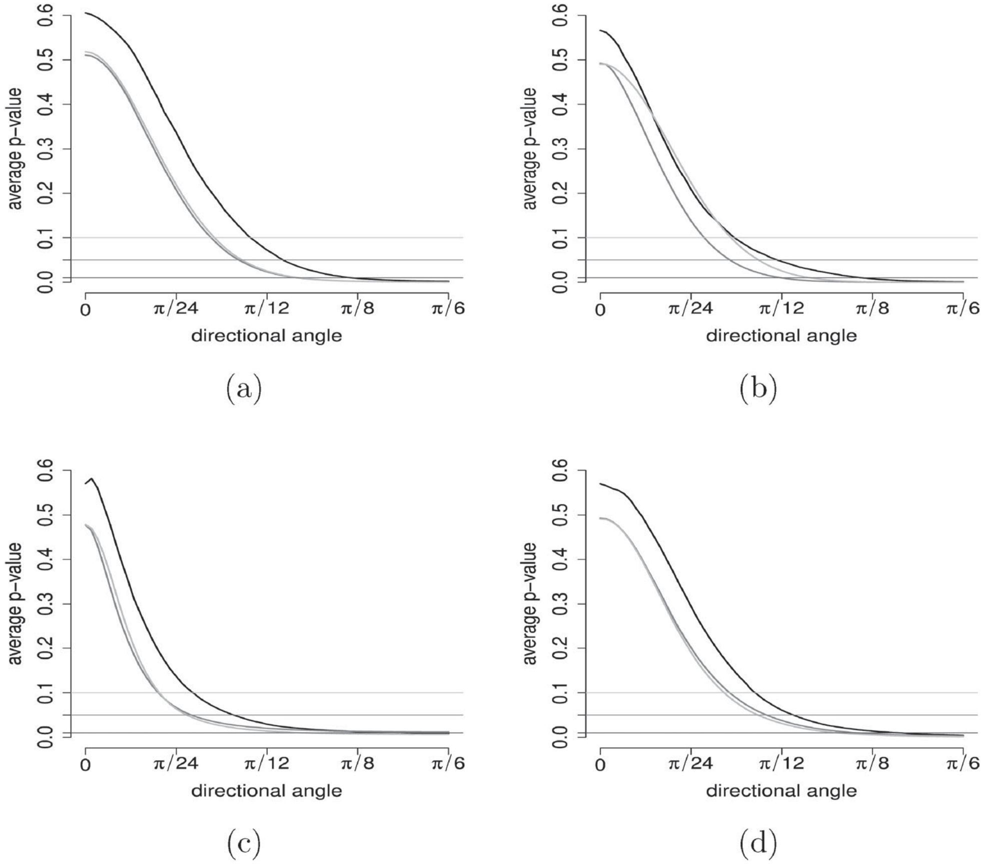

Figure A1. Comparison between T_{sup}, T_N and T_W for distributions with independent marginals. The figure shows the averages of sample p-values coming from the tests T_{sup} (black), T_N (dark gray) and T_W (light gray) of axial symmetry around a line in direction $\mathbf{u} = (\cos(\alpha), \sin(\alpha), 0)^\top$ for $\alpha \in [0, \pi/6]$. The plots have been obtained from 1000 independent samples containing $n = 100$ independent observations $(Y_1, 2Y_2, 3Y_3)^\top$ with independent marginals where Y_i's, $i = 1, \ldots, 3$, are (a) standard normal, (b) uniform on (0, 1), (c) standard exponential, and (d) standard logistic.

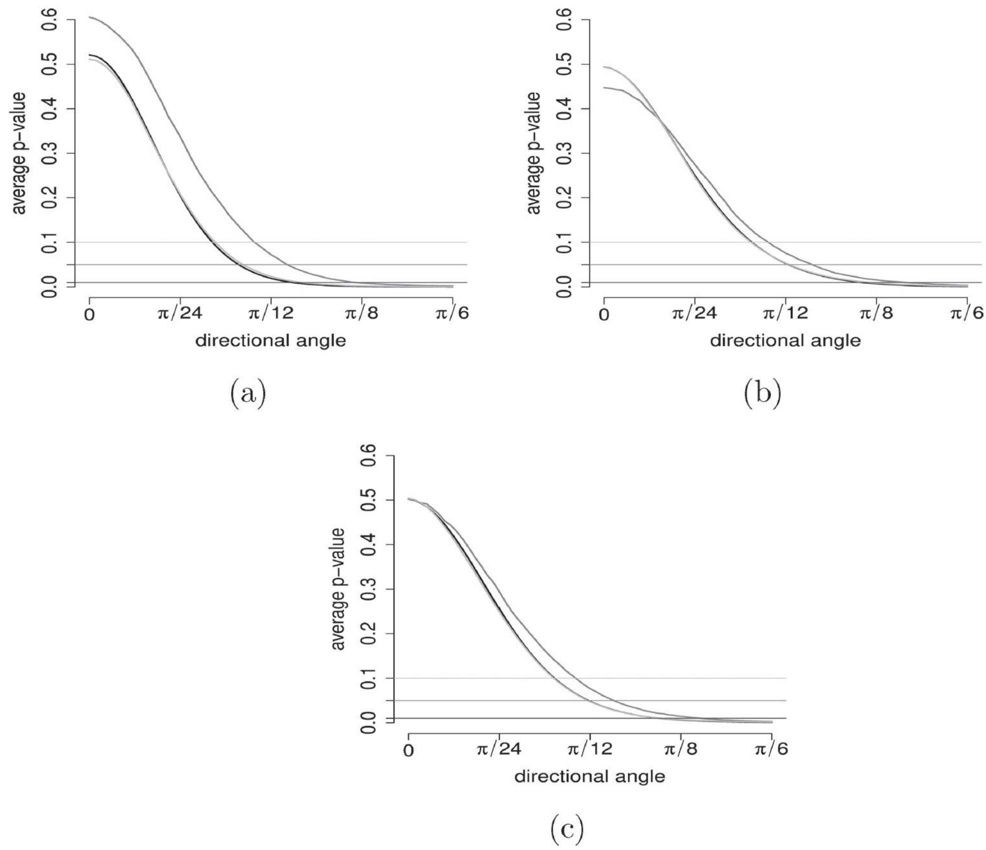

Figure A2. Comparison between T_C, T_{sup} and T_N for elliptical distributions. The figure shows the averages of sample p-values coming from the tests T_C (black), T_{sup} (dark gray) and T_N (light gray) of axial symmetry around a line in direction $\mathbf{u} = (\cos(\alpha), \sin(\alpha), 0)^\top$ for $\alpha \in [0, \pi/6]$. The plots have been obtained from 1000 independent samples containing $n = 100$ independent observations $(Y_1, 2Y_2, 3Y_3)^\top$ where the distribution of $(Y_1, Y_2, Y_3)^\top$ is (a) multivariate standard normal, (b) multivariate canonical Laplace, or (c) multivariate canonical Student with 7 degrees of freedom. Note that T_{sup} is formally justified only in (a) and that the results for T_C and T_N almost coincide.

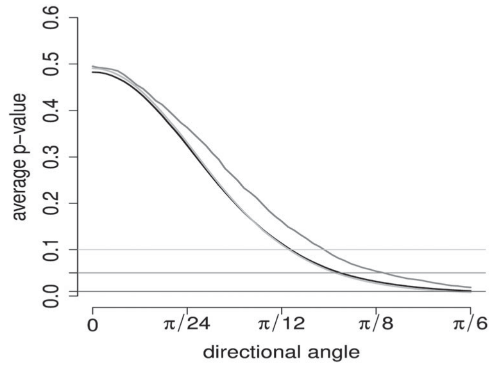

Figure A3. Comparison between T_N, T_S and T_W for multivariate normal distribution. The figure shows the averages of sample p-values coming from the tests T_N (black), T_S (dark gray) and T_W (light gray) of axial symmetry around a line in direction $\mathbf{u} = (\cos(\alpha), \sin(\alpha), \mathbf{0}^\top)^\top$ for $\alpha \in [0, \pi/6]$. The plots have been obtained from 1000 independent samples containing $n = 100$ independent ten-dimensional observations $(Y_1, 2Y_2, \ldots, 10Y_{10})^\top$ where the distribution of $(Y_1, \ldots, Y_{10})^\top$ is multivariate standard normal. The results for T_N and T_W almost coincide.

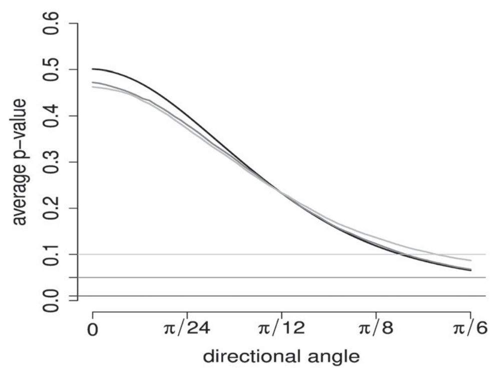

Figure A4. Comparison between T_C, T_R and T_N for small normal samples. The figure shows the averages of sample p-values coming from the tests T_C (black), T_R (dark gray) and T_N (light gray) of axial symmetry around a line in direction $\mathbf{u} = (\cos(\alpha), \sin(\alpha), 0)^\top$ for $\alpha \in [0, \pi/6]$. The plots have been obtained from 1000 independent samples containing $n = 25$ independent observations $(Y_1, 2Y_2, 3Y_3)^\top$ where the distribution of $(Y_1, Y_2, Y_3)^\top$ is multivariate standard normal.

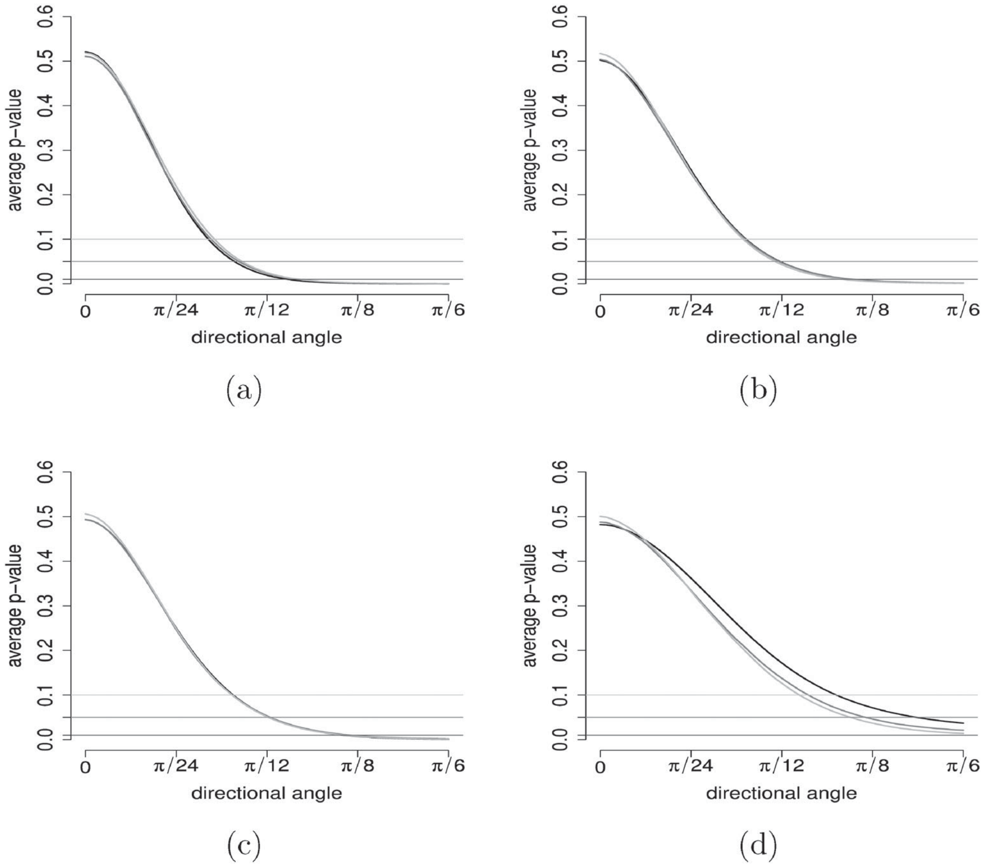

Figure A5. Comparison between T_C, T_N and T_W for elliptical distributions with finite sixth moments. The figure shows the averages of sample p-values coming from the tests T_C (black), T_N (dark gray) and T_W (light gray) of axial symmetry around a line in direction $\mathbf{u} = (\cos(\alpha), \sin(\alpha), 0)^\top$ for $\alpha \in [0, \pi/6]$. The plots have been obtained from 1000 independent samples containing $n = 100$ independent observations $(Y_1, 2Y_2, 3Y_3)^\top$ where the distribution of $(Y_1, Y_2, Y_3)^\top$ is (a) multivariate standard normal, (b) multivariate canonical Student with 7 degrees of freedom, (c) multivariate canonical Laplace, or (d) multivariate canonical power exponential with kurtosis parameter $\kappa = 0.2$.

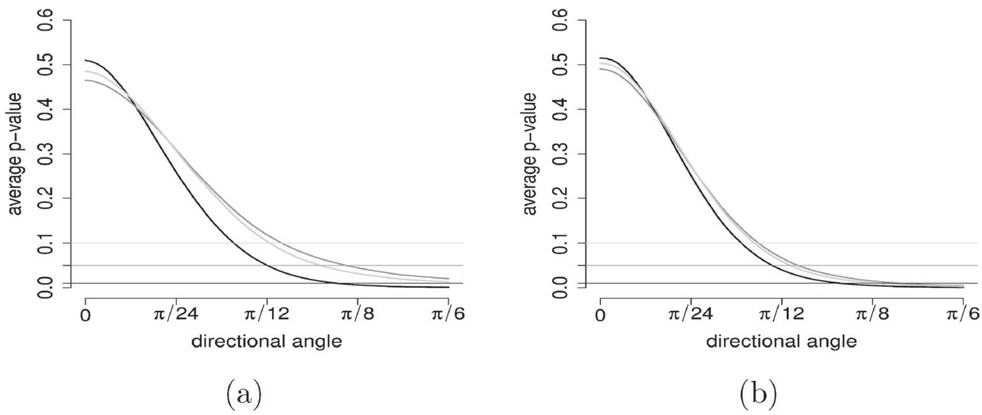

Figure A6. Comparison between T_R, T_N and T_W for heavy-tailed elliptical distributions. The figure shows the averages of sample p-values coming from the tests T_R (black), T_N (dark gray) and T_W (light gray) of axial symmetry around a line in direction $\mathbf{u} = (\cos(\alpha), \sin(\alpha), 0)^\top$ for $\alpha \in [0, \pi/6]$. The plots have been obtained from 1000 independent samples containing $n = 100$ independent observations $(Y_1, 2Y_2, 3Y_3)^\top$ where the distribution of $(Y_1, Y_2, Y_3)^\top$ is multivariate canonical Student with (a) 3 or (b) 5 degrees of freedom.

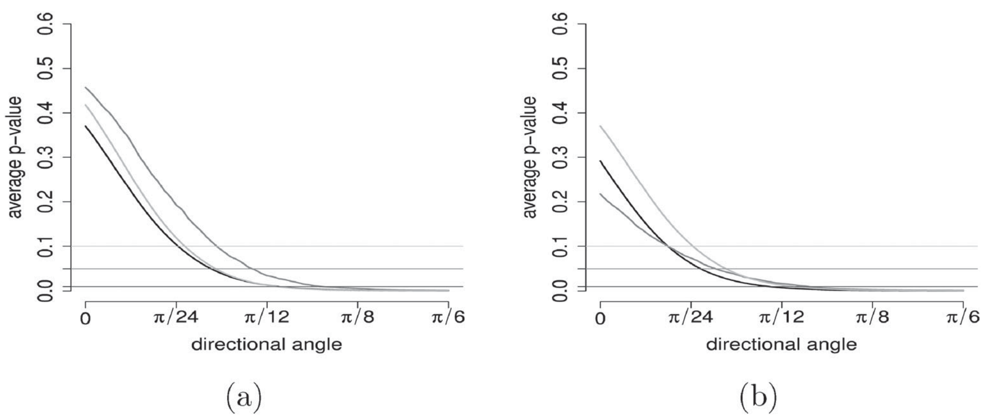

Figure A7. Sensitivity of T_C, T_{sup}, T_N, T_S and T_W to outliers for contaminated normal distribution. The figure shows the averages of sample p-values coming from the tests (a) T_N (black), T_S (dark gray) and T_W (light gray) or (b) T_C (black), T_{sup} (dark gray), T_N (light gray) of axial symmetry around a line in direction $\mathbf{u} = (\cos(\alpha), \sin(\alpha), 0)^\top$ for $\alpha \in [0, \pi/6]$. The plots have been obtained from 1000 independent samples containing $n = 100$ independent three-dimensional observations $(Y_1, 2Y_2, 3Y_3)^\top$ where the distribution of $(Y_1, Y_2, Y_3)^\top$ is multivariate standard normal but each coordinate of the first two observations is increased by 3.

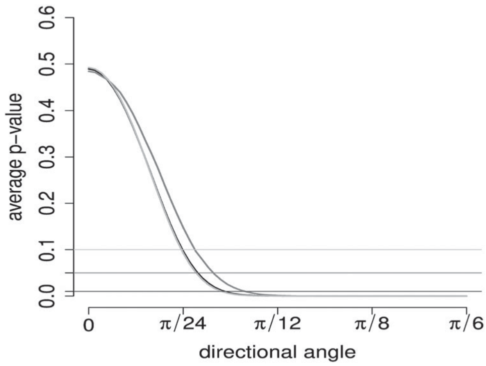

Figure A8. Comparison of T_N, T_S and T_W for large large-dimensional normal samples. The figure shows the averages of sample p-values coming from the tests T_N (black), T_S (dark gray) and T_W (light gray) of axial symmetry around a line in direction $\mathbf{u} = (\cos(\alpha), \sin(\alpha), \mathbf{0}^\top)^\top$ for $\alpha \in [0, \pi/6]$. The plots have been obtained from 1000 independent samples containing $n = 1000$ independent observations $(Y_1, 2Y_2, \ldots, 100Y_{100})^\top$ of dimension $m = 100$ where the distribution of $(Y_1, \ldots, Y_{100})^\top$ is multivariate standard normal. The results for T_N and T_W virtually coincide.

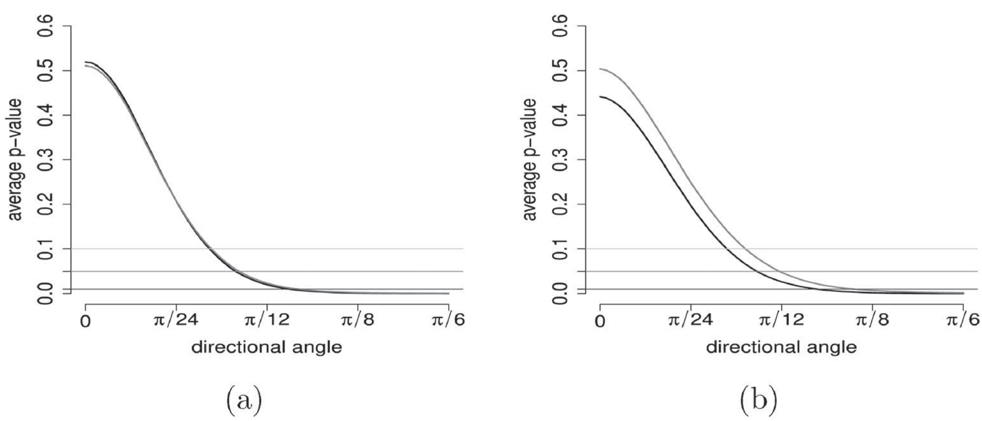

Figure A9. Comparison of T_{N0} and T_N using different variance matrix estimators. The figure shows the averages of sample p-values coming from the tests T_{N0} (black) and T_N (dark gray) of axial symmetry around a line in direction $\mathbf{u} = (\cos(\alpha), \sin(\alpha), 0)^\top$ for $\alpha \in [0, \pi/6]$. The plots have been obtained from 1000 independent samples containing $n = 100$ independent three-dimensional observations $(Y_1, 2Y_2, 3Y_3)^\top$ where the distribution of $(Y_1, Y_2, Y_3)^\top$ is (a) multivariate standard normal or (b) multivariate canonical Student with 7 degrees of freedom.

Appendix 3. Tables

Table A1. Test comparison in the bivariate case.

Testing bivariate symmetry around the *x*-axis I										
	H_0^{UNI}					$H_0^{\mathrm{BVN}(0)}$				
$n =$	50	60	75	100	150	50	60	75	100	150
T_{N0}	0.051	0.051	0.050	0.049	0.050	0.051	0.051	0.051	0.051	0.050
T_N	0.053	0.052	0.052	0.050	0.051	0.050	0.051	0.051	0.051	0.050
T_{S0}	0.052	0.052	0.049	0.050	0.050	0.052	0.051	0.050	0.052	0.050
T_S	0.054	0.054	0.049	0.051	0.051	0.054	0.053	0.050	0.053	0.051
T_{W0}	0.052	0.051	0.051	0.051	0.050	0.051	0.051	0.052	0.052	0.050
T_W	0.051	0.050	0.051	0.050	0.050	0.049	0.050	0.051	0.051	0.050
$RR_{k=2}$	0.04	0.05	0.04	0.04	0.06	0.04	0.05	0.04	0.05	0.05
$RR_{k=5}$	0.06	–	0.04	0.04	0.03	0.05	–	0.03	0.03	0.05
EG	0.03	0.04	0.04	0.04	0.05	0.04	0.03	0.03	0.04	0.04
	$H_1^{\mathrm{BVN}(0.3)}$					$H_1^{\mathrm{BVN}(0.6)}$				
T_{N0}	0.566	0.646	0.746	0.861	0.963	0.997	0.999	1.000	1.000	1.000
T_N	0.536	0.621	0.725	0.847	0.959	0.995	0.999	1.000	1.000	1.000
T_{S0}	0.395	0.461	0.553	0.679	0.847	0.963	0.985	0.996	1.000	1.000
T_S	0.402	0.467	0.553	0.682	0.849	0.964	0.986	0.996	1.000	1.000
T_{W0}	0.553	0.632	0.732	0.848	0.957	0.996	0.999	1.000	1.000	1.000
T_W	0.523	0.607	0.711	0.835	0.953	0.994	0.999	1.000	1.000	1.000
$RR_{k=2}$	0.18	0.27	0.29	0.39	0.55	0.73	0.86	0.94	0.97	1.00
$RR_{k=5}$	0.17	–	0.25	0.36	0.56	0.74	–	0.93	0.98	1.00
EG	0.07	0.08	0.011	0.16	0.24	0.36	0.47	0.61	0.80	0.95

Notes: Six variants of the test of (5), namely T_{N0}, T_N, T_{S0}, T_S, T_{W0}, and T_W, are compared in terms of empirical size and power to the RR_k test (with bin parameter $k = 2$ or $k = 5$) of Rao and Raghunath (2012) and to the central symmetry EG test of Einmahl and Gan (2016) used for testing axial symmetry as described in Riahi and Patil (2021). All cases use sample sizes $n = 50, 60, 75, 100$ and 150, two null hypotheses (H_0^{UNI} and $H_0^{\mathrm{BVN}(0)}$) of symmetry around the *x*-axis and two alternatives ($H_1^{\mathrm{BVN}(0.3)}$ and $H_1^{\mathrm{BVN}(0.6)}$). The results for $RR_{k=2}$, $RR_{k=5}$ and EG tests, based on 1000 replications, are copied directly from Riahi and Patil (2021) for maximum reliability. The other figures were obtained from 100, 000 simulation experiments.

Table A2. Consistency.

Testing bivariate symmetry around the *x*-axis II										
	H_1^{UXM}					H_1^{HAM}				
$n =$	50	60	75	100	150	50	60	75	100	150
T_{N0}	0.051	0.049	0.050	0.050	0.051	0.050	0.050	0.052	0.050	0.051
T_N	0.046	0.045	0.047	0.047	0.049	0.045	0.046	0.047	0.048	0.048
T_{S0}	0.048	0.048	0.048	0.049	0.050	0.050	0.049	0.048	0.050	0.050
T_S	0.051	0.050	0.048	0.050	0.051	0.053	0.051	0.048	0.051	0.051
T_{W0}	0.050	0.049	0.049	0.050	0.051	0.050	0.049	0.049	0.050	0.050
T_W	0.046	0.046	0.047	0.048	0.050	0.045	0.046	0.047	0.048	0.049

Notes: The tests T_{N0}, T_N, T_{S0}, T_S, T_{W0}, and T_W need not be consistent against all possible alternatives, which is illustrated (for various sample sizes *n*) with their empirical powers against two special alternatives (H_1^{UXM} and H_1^{HAM}) taken from Riahi and Patil (2021).